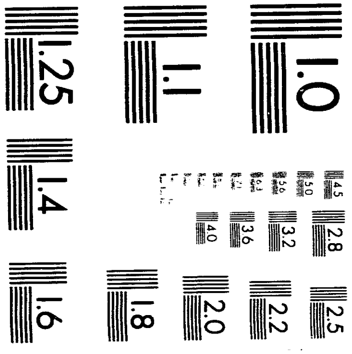
1.0
1.1
1.25
1.4
1.6
1.8
2.0
2.2
2.5
2.8
3.2
3.6
4.0
4.5
5.0
5.6

1 of 1

CONF-931009--13

IS-M 776

LIQUID AND SOLID SOLUBILITY OF Ag IN $Bi_2Sr_2CaCu_2O_8$

R. W. McCallum, K. W. Dennis, L. Margulies, and M. J. Kramer

Ames Laboratory,
Iowa State University
Ames, IA 50011

Abstract

Currently, the leading candidates for usable high temperature superconducting wires are Bi-Sr-Ca-Cu-O tapes produced by modifying the powder in tube process. In order to obtain crystallographic texture, these tapes are processed by partial melting then slow cooling through the peritectic. While it is well known that Ag suppresses the lowest liquidus temperature of the Bi based materials, no serious investigation of the Bi-Sr-Ca-Cu-O-Ag phase diagram has been undertaken. Solubilities of Ag in Bi2212 melt was determined by ICP-AES and TEM/EDS on samples of Bi2212 and 20 wt.% Ag which were melt-spun in air at temperatures of 900 to 1200°C. The most prominent feature of the phase diagram was found to be a liquid immiscibility at all temperatures. There exists a eutectic on each side of this gap. For the Ag rich side the eutectic is at 98 at.% Ag and depresses the melting by 15°C over that for pure silver for the same oxygen partial pressure. The oxide rich eutectic contains no more than 4 at.% Ag and depresses the solidus by 30°C. The solid solubility of Ag in Bi-Sr-Ca-Cu-O glass (oxide glass) is found to be less than the detection limits of TEM/EDS and Ag is systematically excluded from the oxide glass.

SUBMITTED TO THE 1993 FALL TMS MEETING

MASTER

ok

Introduction

Currently, the leading candidates for usable high temperature superconducting wires are Bi-Sr-Ca-Cu-O tapes produced by modifying the powder in tube process. In order to obtain crystallographic texture, these tapes are processed by partial melting then slow cooling through the peritectic. There exist in the literature numerous, sometime conflicting, reports of the effect of Ag additions to the $Bi_2Sr_2CaCu_2O_8$ (Bi2212) system. From the standpoint of superconductivity, it has been reported that Ag_2O doped Bi2212 prepared via melt-quenching and heat treated in a vacuum shows a decrease in T_c and J_c (1) while others have reported little to no effect on superconducting properties when Ag is added to sintered Bi2212 (2,3). Numerous attempts to introduce Ag inclusions into the superconducting core of these wires have been made both to try and improve flux pinning and mechanical properties. If small Ag precipitates can be formed with Bi2212 grains flux pinning may be enhanced or alternatively, if Ag can be concentrated at the grain boundaries, it may increase both the mechanical behavior and the weak linked nature of the ceramic. Obviously, the effect of Ag on both the mechanical and superconducting properties of Bi2212 will depend on how the Ag is distributed in the superconducting matrix. As tracer diffusion studies of ^{110}Ag in Bi2212 shows high diffusivity rates in the a-b plane (4), the amount of Ag that goes into the Bi2212 structure, then, will be limited solely by its solubility. While it is well known that Ag suppresses the lowest liquidus temperature of the Bi based materials, no serious investigation of the Bi-Sr-Ca-Cu-O-Ag phase diagram has been undertaken. A detailed knowledge of the Ag-Bi2212 phase diagram is important in recognizing the inherent limitations on Ag-Bi2212 compounds and how they should be processed. When considering the Bi-Sr-Ca-Cu-O-Ag phase diagram, the oxygen partial pressure dependence of the Bi2212 and Bi2212+Ag thermal events must be considered (5).

Experimental Procedures

In order to determine the high temperature solubility of Ag in a Bi2212 melt, samples were quenched from the temperature of interest by chill block melt spinning. Melt-spinning charges were prepared by blending Kalichemie $Bi_2Sr_2CaCu_2O_x$($< 30\mu m$) with 20 wt% Ag powder($< 5\ \mu m$) then pressing into powder pellets for ease of handling and greatest contact of components. SiO_2 was used as crucible material at 1100°C and below and Al_2O_3 was used at 1100°C and above. Orifice diameters ranged from 1.0 mm at lower temperatures to 0.85mm at higher temperatures to control self-purging of the charge due to viscosity changes. All melt-spinning was performed in air. Direct radio-frequency (RF), at 450kHz, induction heating of the pellets was unsuccessful, as the silver would melt, segregate and flow without conductively heating the ceramic oxide sufficiently enough to melt. Charges were, therefore, heated radiantly using an Inconel susceptor heated by RF. This susceptor also acted as a shielding antenna, eliminating RF noise from the thermocouple signal and excluding direct RF heating of the charge. Temperature was monitored simultaneously by a K-type thermocouple in a SiO_2 sheath embedded in the melt and by a two-color infared pyrometer aimed at the susceptor. On reaching the desired temperature, the molten stream was quenched onto a copper chill block, at ambient temperature, rotating at 20 meters per second. Ejection pressures were 3 - 4 psi.

TEM was performed using a Philips CM30 at 300kV equipped with a Be window energy dispersive detector (EDS). The samples were prepared by floating lightly ground ribbon pieces in ethanol onto a gold grid. Thermal analyses were done on lightly ground ribbon pieces using a Perkin-Elmer DTA1700 in flowing (50 cc/min.) dry CO_2-free air Chemical analyses were performed using ICP-AES on ribbon pieces which had been optically examined at 50x to assure separation of product types. However, this was not always possible.

Results

Melt-Spinning

In initial experiments, it was observed that in cases where after reaching temperature, the Ag-Bi2212 melt failed to shoot from the crucible, the solidified melt consisted of a Ag nodule at the bottom of the crucible surrounded by oxide material. This suggests an extremely low solid solubility of Ag in Bi2212 melt. Following optimization of the furnace parameters, the melt spun material that resulted from a run could be separated into two distinct types. Long lengths of Ag ribbon (10 - 50 cm) were thrown into a collection tube. Of these ribbons, some showed a double-sided morphology. The remainder of the ribbons were nearly purely metallic with small streaks of oxide glass near the ribbon edges. It seems clear that the double sided ribbons resulted from a phase separated liquid stream. It is not clear, though, if the oxide glass seen on the metal ribbons was due to separation in the liquid or subsequent separation upon solidification. The second distinct type of melt-spun material was a oxide glass flake, 5 - 10 mm in length. The oxide glass flakes were thrown off the wheel at a lower trajectory than the metal ribbons, and as a result did not land in the collection tube. Instead the oxide glass flakes collected in the wheel chamber. Often, a large clump of tangled oxide glass ribbon would collect just below the opening to the collection tube. XRD analysis of this material showed significant crystallinity.

ICP-AES

Chemical analysis of the oxide and metal ribbons are presented in Table 1. The oxide ribbons show an increase in Ag content from 6.1 at. % at 900°C to 9.8% at 1200°C. The two samples processed at 1100°C showed anomalously low Ag contents of 6.3% and 4.9%. In both these cases the ribbons agglomerated, which may have resulted in a slow quench and possible phase separation, explaining the lower Ag contents. The Bi content of the oxide ribbons steadily decreased with increasing temperature from 30% at 900°C to 24% at 1200°C. Similarly, the Cu content decreased from 28% at 900°C to 25.2% at 1200°C. The Sr and Ca content of the oxide ribbons showed little systematic variation with temperature. The Si and Al contamination was minimal for samples processed in quartz, while samples processed in Al_2O_3 showed 4.5% Al and 0.3-2.1% Si in the oxide ribbons and negligible Si and Al content in the metal ribbons. The metal ribbons showed a decrease in Ag content with increasing temperature from 99% at 950°C to 96.8% at 1200°C. Again, the samples processed at 1100°C gave slightly anomalous results. Finally, the amount of Cu in the metal ribbons increased with temperature from 0.8% at 950°C to 2.2% at 1200°C. This may reflect an increasing tendency to form metallic Cu with increasing temperature, which in turn is soluble in Ag.

TABLE 1. ICP analysis, in mole % and cation ratio of Bi:Sr:Ca:Cu with Cu fixed at 2, of the precursor Bi2212, oxide ribbons, and metal ribbons. Mole percentages are accurate to 1 to 3% relative.

	MOLE %							
	Bi	Sr	Ca	Cu	Ag	Si	Al	Bi/Sr/Ca/Cu
PRECURSOR								
	25.5	27.2	13.5	27.2	-	-	-	1.88/2.00/1.00/2.00
OXIDE RIBBONS								
Temp(C)								
900	30.0	24.5	11.2	28.0	6.1	0.1	0.0	2.14/1.75/0.80/2.00
950	28.4	24.8	12.5	26.4	7.6	0.2	0.1	2.15/1.87/0.95/2.00
1000	28.4	24.0	12.4	27.6	7.5	0.1	0.0	2.05/1.74/0.90/2.00
$1100^{\#}$	28.0	25.2	12.7	27.5	6.3	0.3	0.0	2.04/1.84/0.93/2.00
$1100^{*\#}$	24.7	25.2	12.7	25.9	4.9	2.1	4.5	1.91/1.95/0.98/2.00
1200^{*}	24.0	23.5	11.7	25.2	9.8	0.3	4.6	1.99/1.86/0.93/2.00
METAL RIBBONS								
950	0.0	0.0	0.0	0.8	99.0	0.0	0.0	0.00/0.00/0.00/2.00
1000	0.3	0.2	0.1	1.2	98.2	0.0	0.0	0.50/0.33/1.68/2.00
$1100^{\#}$	0.1	0.0	0.0	1.2	98.6	0.0	0.0	0.17/0.00/0.00/2.00
$1100^{*\#}$	0.4	0.2	0.1	4.4	94.9	0.0	0.0	0.18/0.09/0.05/2.00
1200^{*}	0.3	0.3	0.2	2.2	96.8	0.1	0.1	0.27/0.27/0.18/2.00

* in Al_2O_3 crucible with thermocouple

\# Ribbons aglomerated, resulting in a slow quench and possible phase separation.

DTA

Differential thermal analyses (DTA) were done on product ribbons to determine melting events and, therefore, invariant points on the pseudo-binary phase diagram. The DTA curve of the Ag-rich flake from the melt-spin run at 950°C showed an onset of the liquidus at 933°C in air (Fig. 1). This compares to the onset of the liquidus of pure silver in air at 947°C. The suppression of onset temperature is indicative of a eutectic between Ag and the Bi2212 component. The DTA curve of the Bi2212-rich oxide glass flake from the melt-spin run at 950°C showed much more complex melting events (Fig. 2). The endothermic event defining the liquidus deviates from the baseline as low as 810°C with an initial onset of 830°C. This is followed by a compound melting event indicative of two, and probably more, phase boundaries being crossed. Normally, a melting event may occur over a 10 to 15°C range, but this one occurs over at least a 75°C range, corroborating the assumption that this complex peak represents a number of phase fields being crossed. An endothermic event also occurs at an onset of 935°C, which corresponds quite well with the measured onset temperature of the Ag-rich flakes. The 935° endotherm further demonstrates the low solubility of Ag into Bi2212.

TEM

The oxide rich ribbons from the 1000°C run were examined using TEM. The material is a two-phase mixture of an oxide glass matrix with inclusions of Ag (Fig. 3). The inclusions of crystalline Ag varied from 5 nm to 50 nm and tend to be spherical. EDS of the matrix region between the Ag particles showed no Ag while amounts of the ceramic oxide elements, in stoichiometric proportions, was variable when the probe was placed on a Ag particle. This variation scaled inversely with the Ag particle size. The lack of Ag in the spectra for the glass matrix puts the solubility limit of Ag into the oxide glass to < 1 %. The variation in Ag particle size most likely reflects variation in quench rates across the ribbon. These observations strongly suggest that the affinity of Ag for the oxide ceramic is very low.

Discussion

To deal correctly with the Bi-Sr-Ca-Cu-O-Ag phase diagram it is necessary to consider the consequences of a six component system. For such a system, the number of phases plus the number of degrees of freedom is seven. Restricting ourselves to atmospheric pressure, one degree of freedom is eliminated. Thus, five phases are in equilibrium at a fixed temperature if the compositions of all five phases are fixed. As it is beyond the scope of this paper to deal with a six dimensional phase diagram, we will consider a schematic pseudo-binary isopleth through the Bi2212 - Ag system (Fig. 4). In this isopleth we must make the approximation that both end points are components, that is that they are either elements or congruently melting compounds. As we know that this is not the case for Bi2212, this representation will not follow the normal rules for binary phase diagrams. In particular, the compositions of all phases presented in the diagram do not lie in the plane of the isopleth and the lever law is not valid for the individual oxide phases. Starting with the Bi2212 compound, we know from the high temperature x-ray work of Ming Xu et. al. (6) that Bi2212 decomposes to $(Sr_{1-x}Ca_x)CuO_2$ (11)+ liquid to $(Sr_{1-x}Ca_x)_2CuO_3$ (21) + liquid

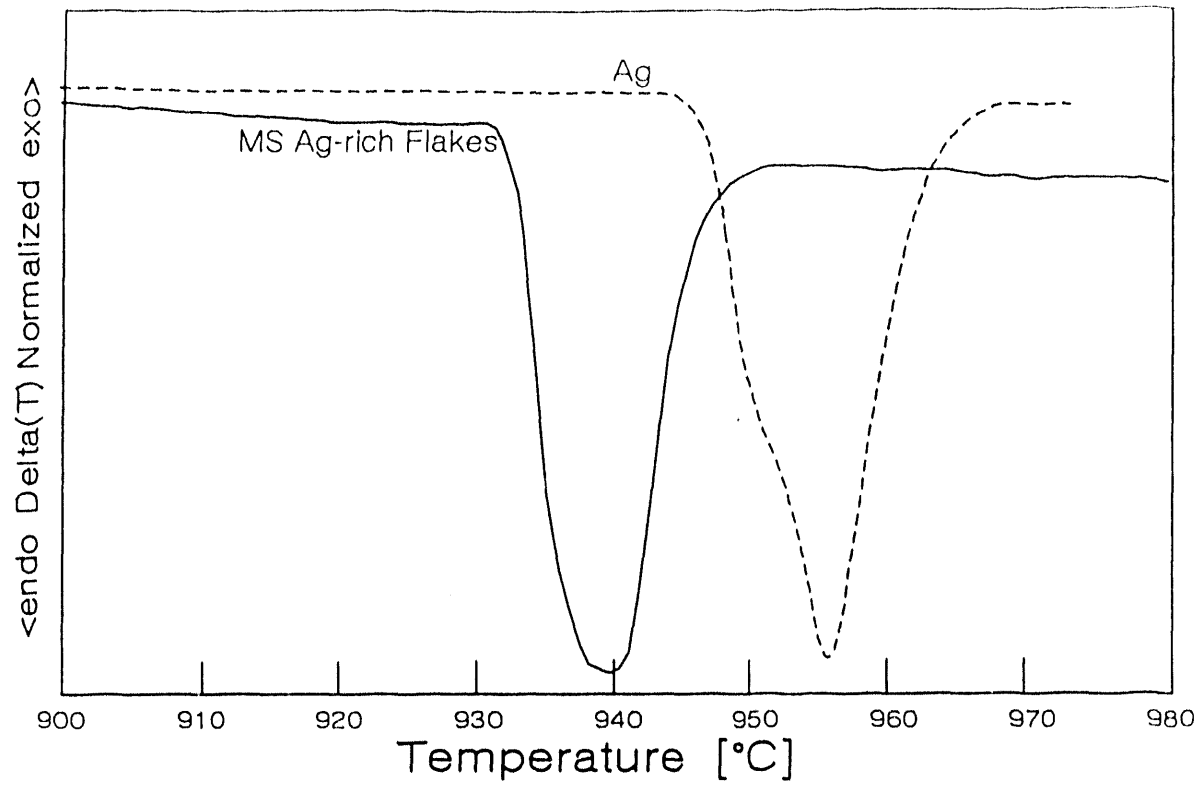

Figure 1 - DTA of Ag-rich ribbon pieces from the 950°C melt-spin run.

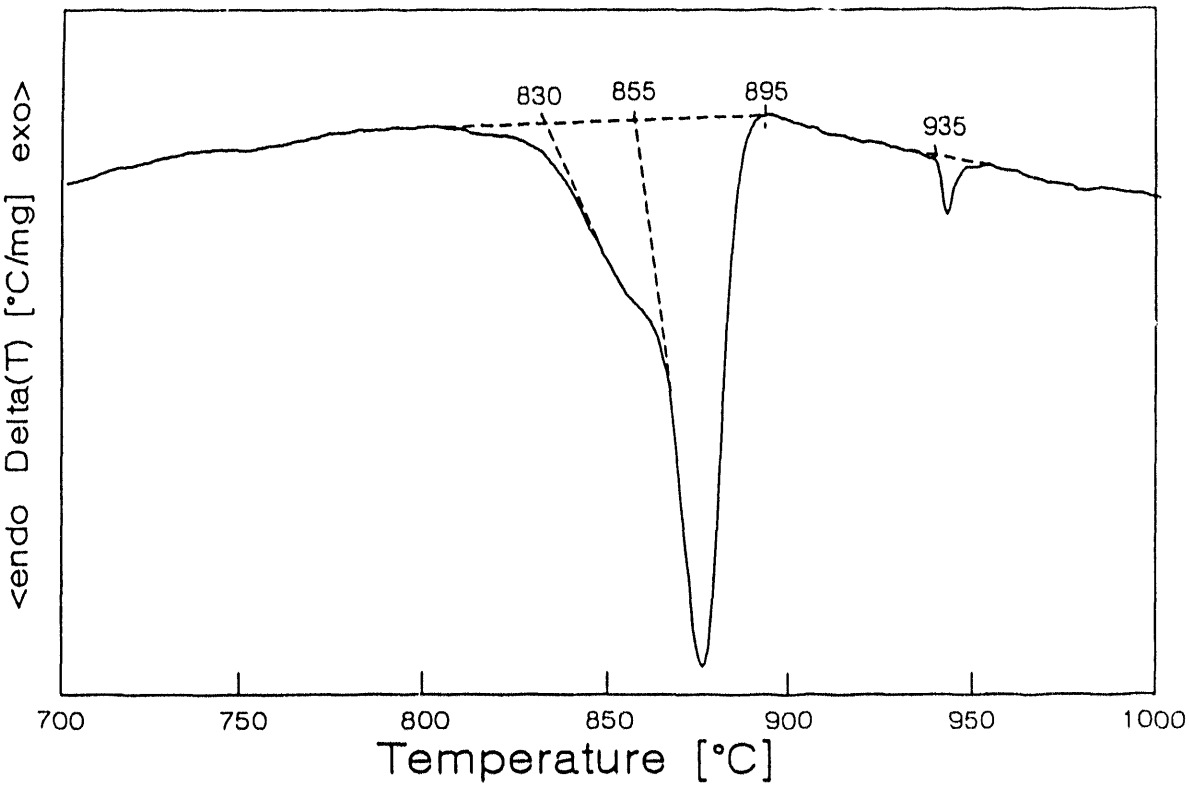

Figure 2 - DTA of oxide-rich glass ribbon pieces from the 950°C melt-spin run.

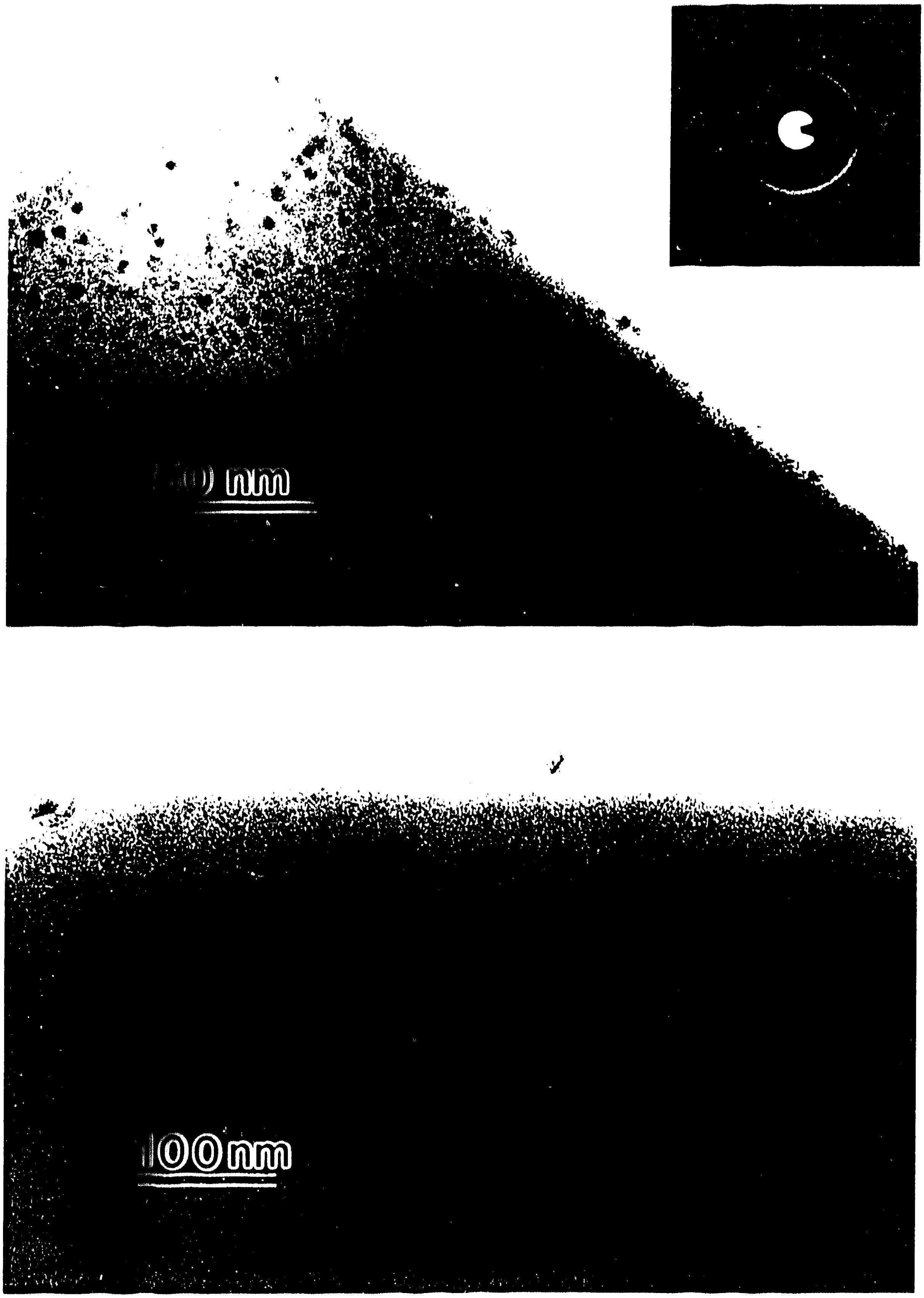

Figure 3 TEM micrograph of the 1000°C oxide flakes showing the variability in distribution of the Ag precipitates within the glassy matrix. The broad ring in selected area diffraction pattern indicates the oxide is fully amorphous but the discrete spots index to Ag, indicating the Ag is crystalline.

to $(Sr_{1-x}Ca_x)O$ (10) + liquid and final completely melts. Using the phase rule, it is possible to derive that when another component is added to the system, the lines separating the two phase regions become three phase regions as we move into our pseudo-binary isopleth. As a consequence, between the liquidus and the Bi2212 + Ag solidus we pass through seven different two, three and four phase regions within a space of approximately 80°C. As the differentiation of these regions is beyond the resolution of the current experiment, the 11, 21 and 10 phases will all be lumped together as OX meaning solid oxide phases (Fig. 4).

The main feature of the diagram is the large liquid immiscibility between the oxide and Ag liquids which is clearly demonstrated by the segregation of Ag and Bi2212 melt in the air quenched crucible. As demonstrated by the two types of flake obtained on melt spinning, the segregation was such that the composition at the limits of immiscibility for both sides of the region could be obtained from a single run at fixed temperature. On the Bi2212 side of the region, the slope of the boundary is approximately 1 at.%/100°C, while on the Ag side the slope is somewhat steeper. From this data it is not possible to extrapolate the critical point for the immiscibility region which is well outside the range of the experiments. Since, from drop tube melt spinning in $REBa_2Cu_3O_{7-\delta}$ systems (7), we have determined that at temperatures on the order of 1600 - 1700 °C, CuO begins to reduce to form Cu metal and the melt phase segregates into metallic and oxide melts. Thus, the critical point for the immiscibility will most likely occur in what is essentially a metallic melt. Consistent with this picture is the fact that the Ag rich flake shows increasing amounts of Cu relative to the other oxide constituents with increasing temperature. It is also probable that at atmospheric pressure, the liquid immiscibility terminates not at a critical point, but at the boiling point of the Ag-Cu mixture. From a processing point, this limits the amount of Ag precipitates within the oxide glass to less than ten percent.

From the DTA measurements on both the oxide rich and Ag rich flakes, it is clear that a psuedo-eutectic exists on each side of the diagram. For the oxide rich side the existence of this eutectic has been know for quite some time but the composition at which it occurs has not been extensively investigated. The exact depth of the eutectic is not an easily determined number since it involves a cross section diagram containing an eutectic trough. In order to accurately determine the relative eutectic depth, samples with equal oxygen content must be compared as the effects of oxygen content are at least a factor of five larger than those of Ag (5). Comparing samples with as similar of a thermal history as possible, yields a value of 30°C for this eutetic trough. Extrapolating along liquid immiscibility line gives a Ag composition of 4 at.% for the eutectic. It should be noted that this is an upper limit to the Ag composition, but the lower limit is not well defined as this point.

Extrapolating the liquid immiscibility line on the Ag rich side gives a eutectic composition of 98 at.% Ag. As no additional phase boundaries are crossed, this extrapolation should be valid. The temperature of the eutectic is 15°C below that of pure Ag under identical oxygen conditions.

From a detailed examination of the melt spun oxide rich flakes, it is possible to determine the limits of solid solubility of Ag in the oxide glass. On the micron scale these materials are homogeneous. Therefore chemical analysis or EDS using SEM gives a value determined by the temperature from which the material was quenched. TEM observations reveal that these analyses are misleading. On this scale the Ag segregates into spherical precipitates and the amorphous matrix contains no Ag to the limits of detectability. In situ crystallization of the glass in the TEM (7) indicate that the Ag coarsens at temperatures below the crystallization temperature and given the opportunity, migrates out of the sample. In no case were Ag inclusions found within Bi2212 grains. Determination of the solid solubility of the oxides in Ag has not been done at this time due to the difficulty of preparing TEM samples of the ductile material.

In using the temperatures presented in this phase diagram, one should be cognizant of the fact that both the oxide phases and Ag have reasonable large dependences of their decomposition or melting temperatures on oxygen content (5). While oxygen diffusion in Ag is high near the melting temperature, this is not the case for the oxide materials. The effects of oxygen non-equilibrium are readily observable in processing these materials. Runde et. al. have performed tracer diffusion measurements for oxygen in Bi2212 up to 650°C (8). If one takes the rather risky approach of evaluating the fit they obtained for temperatures near the melting, the time required for oxygen to diffuse 10 microns is of the order of 10 minutes. Clearly the melting temperatures obtained for bulk samples are going to be highly dependent on the exact heating sequence and oxygen partial pressure.

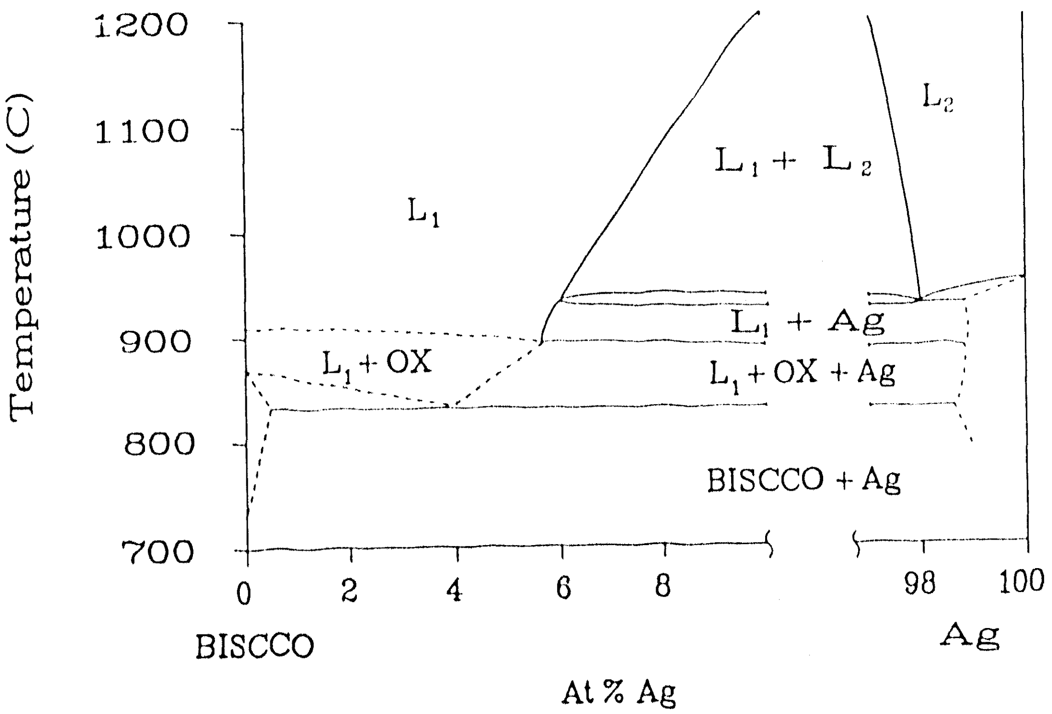

Figure 4 - Simplified pseudo-binary isopleth in the Bi-Sr-Ca-Cu-O-Ag system treating both endpoints as components.

Conclusions

We have demonstrated the existence of a liquid immiscibility gap in the Bi2212+Ag system which covers the region from approximately 8 to 98 at.% Ag. There exists a eutectic on each side of this gap. For the Ag rich side the eutectic is at 98 at.% Ag and depresses the melting by 15°C over that for pure silver for the same oxygen partial pressure. The oxide rich eutectic contains no more than 4 at.% Ag and depresses the solidus by 30°C. The solid solubility of Ag in oxide glass is found to be less than the detection limits of TEM/EDS and Ag is systematically excluded from the Bi2212 during crystallization. All phase transition temperatures in the systems are sensitive to oxygen content and times to reach oxygen equilibrium are long.

Acknowledgments

The work was performed at Ames Laboratory, Iowa State University and was supported by the Director of Energy Research, Office of Basic Sciences, U.S. Department of Energy under Contract No. W-7405-ENG-82

References

1. W. H. Lee, Yoshihiro Abe, and Eikichi Inukai, "Ag_2O-Doped $Bi_2Sr_2Ca_1Cu_2O_x$ Superconductors Prepared via Melt-Quenching," Journal of the American Ceramic Society, 76 (4) (1993), 849-856.

2. T. E. Jones et al., "Effect of silver additions on sintered $Bi_2Sr_2CaCu_2O_8$," Physica C, 201 (1992), 279-288.

3. S. X. Dou et al., "The Interaction of Ag with Bi-Pb-Sr-Ca-Cu-O Superconductor," Physica C, 160 (5-6) (1989), 533-540.

4. Y. Fang et al., "Tracer diffusion of ^{110}Ag in $Bi_2Sr_2CaCu_2O_x$," Applied Physics Letters, 60 (18) (1992), 2291-2293.

5. M.J. Kramer et al. "Effects of oxygen partial pressure of the crystallization pathways of $Bi_2Sr_2CaCu_2O_x$ and $Bi_2Sr_2CaCu_2O_x$+Ag" (in preparation).

6. M. Xu et al., "Investigations of Crystalline Phases in the Melting of $Bi_2Sr_2CaCu_2O_x$,"Applied Superconductivity, 1 (1/2), (1993), 53-60.

7. Work in progress.

8. M. Runde et al. "Tracer diffusion of oxygen in $Bi_2Sr_2CaCu_2O_x$" Physical Review B, 45 (13) (1992), 7375-7382.

DATE

FILMED

1 / 11 / 94

END